

Appendix 4

Doppler Spectroscopy Measurements of Plasma Flow in HSX

A4.0: Introduction

The 1 meter focal length spectrometer used for ion temperature measurements is also, in principle, capable of making impurity flow measurements. These studies have proven difficult; the results to date are described in this appendix.

Section 1 describes the problems associated with the wavelength calibration of the instrument and describes the calibration system designed to alleviate the problems. Section 2 presents preliminary measurements of enhanced C^{+4} rotation in antiMirror discharges. Section 3 provides some discussion and summarizes the results.

A4.1: Wavelength Jitter and Absolute Wavelength Calibration of the Spectrometer

One of the main difficulties with the Doppler spectroscopy measurement in HSX has been excessive "jitter" in the wavelength calibration. This is illustrated in figure A4.1. The Hg line at 296.73nm was shined into the entrance slit of the spectrometer and the exposure recorded every 30 seconds for 360 minutes. The CCD was binned into three regions as is typically used during spectroscopic measurements. Gaussian fits were applied to the data at each exposure, allowing a measurement of the shift of the line center as a function of time. The resulting time traces are shown in figure A4.1, where the three regions are indicated separately.

This graph shows two important features. The top and bottom regions are shifted to larger pixel numbers than the center region. This may be due to line curvature.¹ The second feature to note is the general shift of the set of line centers throughout the day. This leads to a

variation of the wavelength calibration of the instrument during the day. The drift over the day is approximately 1 pixel. With a dispersion of $\sim 4000\mu\text{m}/\text{nm}$ and $26\mu\text{m}$ wide pixels, this drift corresponds to an apparent wavelength shift of $\sim 6.5 \times 10^{-3}\text{nm}$. For light at 227nm , this wavelength shift looks like a Doppler shift corresponding to 7km/s , which is comparable to the largest flow speeds observed in HSX using Doppler spectroscopy.

There are two lessons taken from this data. It is not possible to compare the pixel locations of spectral lines taken on different discharges. Any wavelength shift observed might be the result of plasma flow, or simply due to a change in the wavelength calibration of the instrument. Secondly, the constant ~ 0.1 pixel displacement between the different CCD regions needs to be accounted for when comparing spectra from the three regions of the CCD.

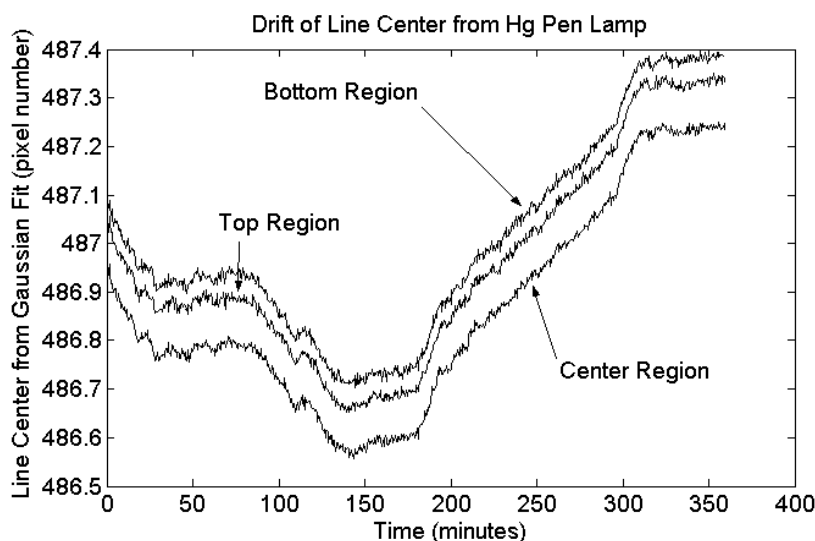


Figure A4.1: Variation in time of the 296.73 Hg line center, showing the wavelength drift of the spectrometer.

A system has been designed with the goal of a proper wavelength calibration on each discharge of HSX. A cadmium lamp has a very bright spectral line at 228.8022nm ,² which is near the C^{4+} spectral lines near 227nm and the C^{+2} line at 229nm . A cadmium lamp³ has been arranged to illuminate a set of 30 optical fibers (Thorlabs FG-365-UEN, $365\mu\text{m}$ core diameter, 0.22NA), as illustrated in figure A4.2. The other ends of these optical fibers are at the collection optics on HSX, with three of these calibration fibers allocated to each collection optics assembly

(recall from Chapter 3 that there are 9 discrete collection optics assemblies on a miniflange array, and a single toroidal view). Light from these three small fibers is input to the collection optics assembly, where it is reflected from the collection lens and vacuum window. This reflected light enters the main fiber bundle that leads to the spectrometer. A photograph of the collection optics assemblies and the calibration fibers is provided in figure A4.3

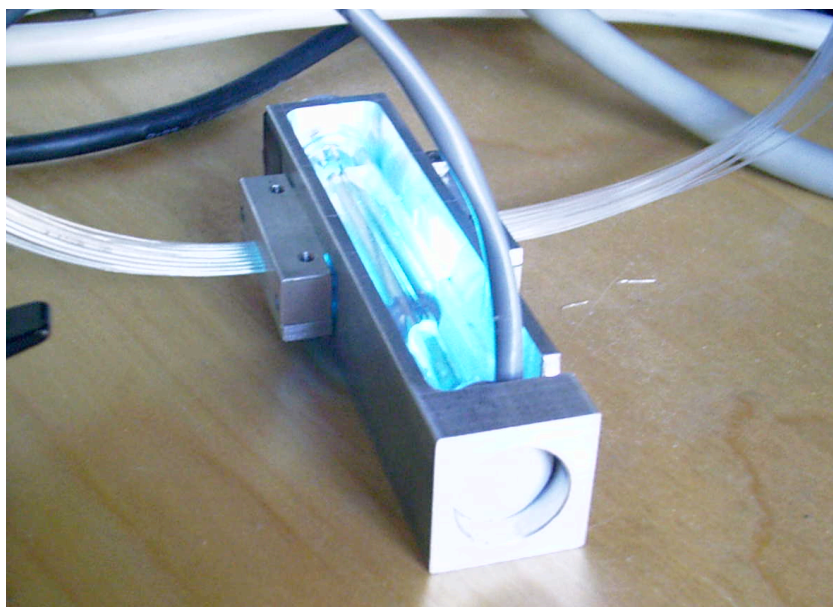


Figure A4.2: Photograph of the Cd lamp with calibration optical fibers.

This system has been integrated into the discharge sequence as follows. The Cd lamp is left on throughout the run day. Before and after each plasma discharge, there are between three and five long CCD exposures taken. The length of ~ 1 second per calibration exposure is necessary so that a sufficient amount of the reflected cadmium light can be collected. Note that the Cd lamp is also on during the discharge, but the short (~ 40 ms) exposure for plasma light is not long enough to accumulate a significant amount of Cd light.

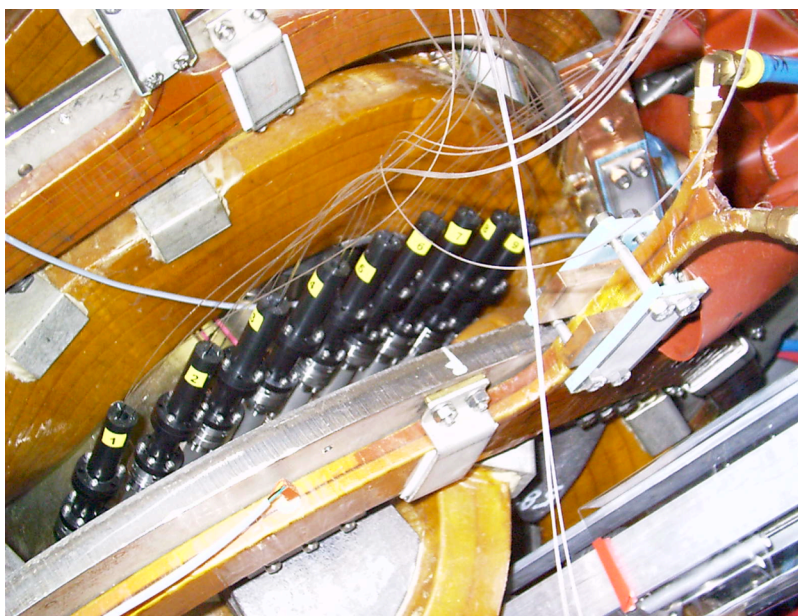


Figure A4.3: Photograph of the collection optics between coils 4 and 5 on field period A. Note the small calibration fibers leading to each of the black Delrin collection optics assemblies.

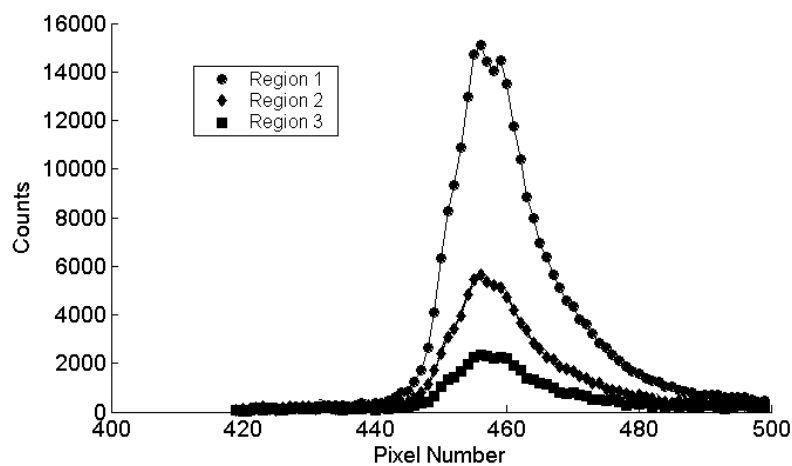


Figure A4.4: Image of the Cd spectral line at $\lambda=228.8$ nm.

An example of the calibration data collected with the system is shown in figure A4.4. Note that this Cd line is not symmetric about its line center; this makes it difficult to interpret the information. Instead of fitting Gaussian functions to these curves to determine the relative shifts between the three regions, a pattern matching technique is used. The data from the top and bottom regions of the CCD are shifted and scaled until they most accurately match the data from

the center region. This provides an estimate of the relative displacements of the three regions. This is repeated for the 6-10 calibration spectra per discharge. The data from the various calibration exposures from a typical discharge are shown in figure A4.5, along with the averages of the 10 calibration spectra. The shifts derived from this method are used to correct for the misalignments of the three regions of the CCD.

It was originally hoped that the Cd spectral line would lead to an accurate wavelength calibration of the instrument, as well as correcting for relative shifts between the regions. This has not proven to be the case. The non-symmetric shape of the spectral line makes it difficult to determine the line center in a way that can be meaningfully compared to the tabulated center wavelength. As a simple means of obtaining unshifted spectral line light for the carbon or oxygen spectral lines of interest, the fiber corresponding to the central region of the CCD is placed on the central chord of the miniflange array. This chord passes through the plasma center in a plane orthogonal to the magnetic axis, and so should detect minimal poloidal or toroidal rotation. The light collected along this chord provides a wavelength reference for the other two chords.

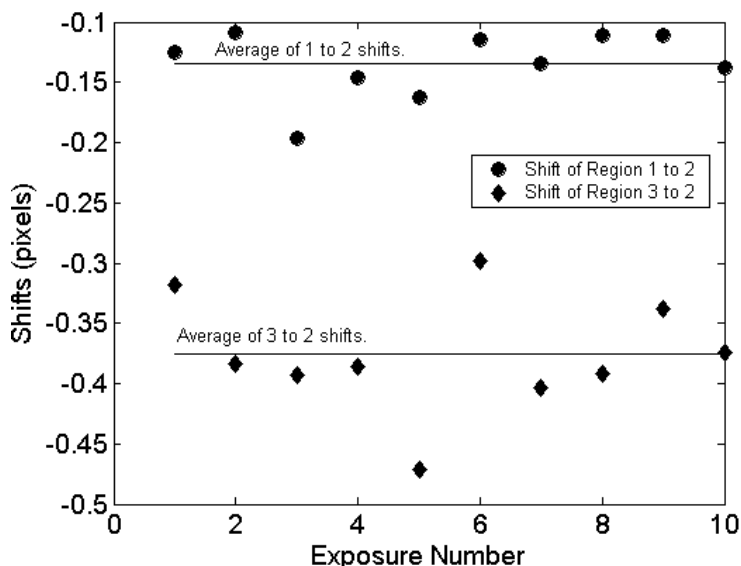


Figure A4.5: Shifts between regions as determined by the Cd lamp system. The exposures correspond to the calibration exposures before and after a discharge.

An example of the reliability of this wavelength calibration system is provided in figure A4.6. The central region of the CCD was illuminated by plasma light from the core chord of the miniflange array. The other two spectrometer channels were on the collection optics chords on either side of the central chord (chords 4 and 6 by the numbering in figure 3.1). These two chords are tangent to approximately the same flux surface. If there is a net poloidal flow, it is anticipated that one chord will be red-shifted with respect to the center chord, while the other is blue shifted by an approximately equal amount.

Two shots were taken in this configuration, and then the two outside fibers were exchanged (between shots 62 and 63), leaving the center fiber untouched. Two more discharges were then taken. The plasma was repeatable over these four discharges. The result of this experiment is shown in figure A4.6. The flow direction measured by the fibers switched signs when the fibers were exchanged, as anticipated. Note that the data are generally displaced toward negative flow speed. This could be due to, for instance, misalignments of the CCD which are not fully accounted for by the Cd calibration system or small non-zero chord integrated flow on the central chord.

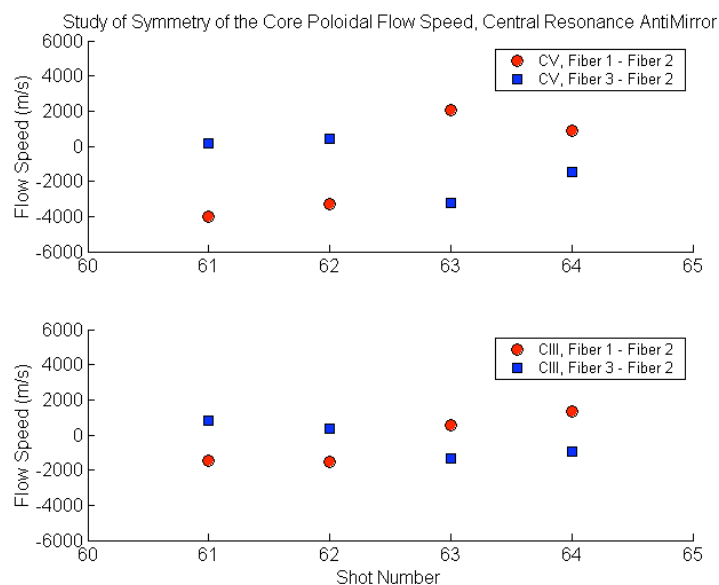


Figure A4.6: Test of the wavelength calibration system by exchanging fibers in similar discharges.

A4.2: Example Measurements of Toroidal Flow in the antiMirror Configuration.

The most interesting flow measurements taken with the spectrometer system were of toroidal flow in the antiMirror configuration of HSX. This data was taken with the plasma heavily doped with methane; approximately 40% of the pressure in the gas system was due to methane. This level of doping was found to be necessary to resolve the carbon light at line average densities $<1 \times 10^{12} \text{ cm}^{-3}$. It is not clear to what extent the substantial methane doping impacted the plasma performance, although the total stored energy was similar to plasmas fueled with pure hydrogen.

The spectrometer was configured with the central region of the CCD collecting light from the central chord of the miniflange array; this light provided the wavelength calibration for the data as described above. One of the remaining two fibers was placed on an adjacent chord of the poloidal array in an attempt to measure core poloidal rotation. The remaining fiber was placed on the toroidal view so as to measure rotation in the toroidal direction.

The line average density was held fixed at $1 \times 10^{12} \text{ cm}^{-3}$ while the antiMirror amp-turn fraction was increased in $\sim 2\%$ increments. The toroidal flow of C^{+4} and C^{+2} from these discharges is shown in figure A4.7. In the QHS configuration, there is only small flow, with both the C^{+4} and C^{+2} flow near zero. As the symmetry is broken, the flow accelerates, reaching a value of almost 10km/s for the C^{+4} species. The value is confirmed for all three C^{+4} spectral lines measured. The C^{+2} also accelerates, going from a slightly negative value to a positive value of $\sim 6\text{km/s}$.

The possible explanation for this observation is as follows. There is a deep minima in $|B|$ in front of the ECH launching window in the antiMirror configuration. This causes a large fraction of the electrons which are heated by the ECH to drift out of the confinement volume.⁴ This drift of high energy electrons constitutes a radial current. Just as in the biased electrode measurements which were the main focus of this dissertation, the radial current of trapped electrons must be compensated for by a return current. This return current induces the rotation which we measure.

The deepening of the local $|B|$ minima with increasing antiMirror fraction leads to a larger loss current.

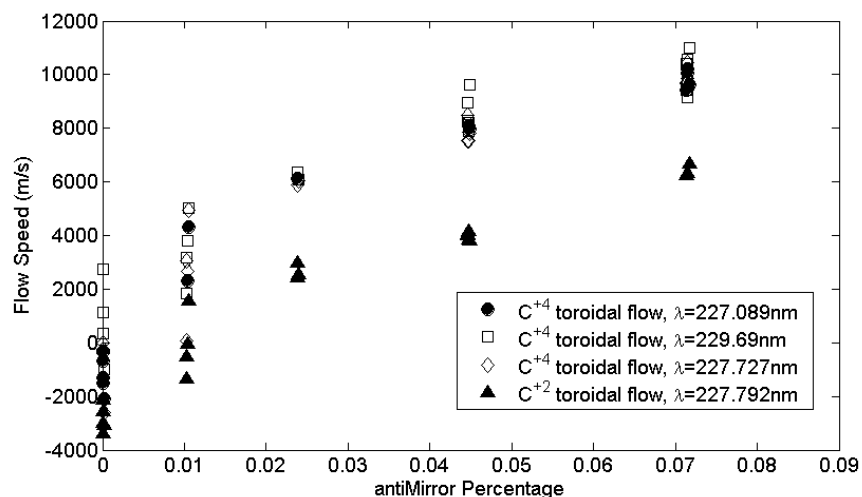


Figure A4.7: Carbon toroidal flow as a function of antiMirror amp-turn fraction.

As a check on the validity of the measurement and interpretation, the experiments were performed with the magnetic field reversed. The toroidal rotation also reversed under these conditions, and had a similar magnitude in the opposite direction. This is consistent with the explanation given above, in the sense that the sign of the radial current would not change, but the magnetic field direction would. The direction of the $\mathbf{J} \times \mathbf{B}$ force is thus reversed.

It is assumed that the spectral line center from the center miniflange chord represents emission with no net Doppler shift. The pixel location of this line center drifts during the day. Figure A4.8 shows the shift of the central chord C⁺⁴ at 227.089nm line center, as a function of shot number. The average line center has been subtracted off. This provides strong evidence that the apparent line shifts observed in figure A4.1 are not due to a simple drift of the pen lamp wavelength, but are related to the spectrometer.

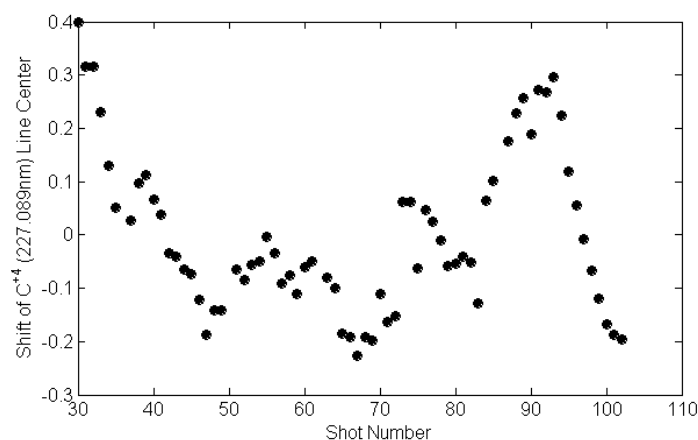


Figure A4.8: Drift of the center of the calibration line throughout a day of data taking.

A4.3: Discussion and Conclusion.

The measurements in this section illustrate that a Doppler spectroscopy system is capable of making measurements of interest in HSX, although a number of concerns have arisen.

The first concern is related to the level of signal. Oxygen light is visible in almost every discharge. There are two arguments against using the O^{+4} line for flow measurements. In the first place, the ionization potential of this state is <100 eV, so it is necessarily an edge species. Secondly, it is not clear what sort of calibration lamp to use to correct for the shifts between regions in the wavelength range near the O^{+4} line at 278nm. The spectral line of the Cd lamp is in this sense perfectly suited for correcting the measurements of the carbon spectral lines. Unfortunately, while the C^{+4} and C^{+2} lines can be observed with the 300 g/mm grating, their signal level is too dim to observe with the 3600 g/mm grating without methane doping.

The relative efficiency of the system with 300 g/mm and 3600 g/mm gratings was measured using an Hg pen lamp. The spectral line at 289.4nm was allowed to shine into the spectrometer after the lamp had been allowed to warm up for 20 minutes. The resulting line profile as measured by the CCD (counts vs. wavelength) was then integrated to determine the total number of counts. This experiment was repeated twice for the 300 g/mm and 3600 g/mm grating. The 300 g/mm grating had a total area under the spectral line of $\sim 5.2 \times 10^5$ count-pixels,

while the 3600 g/mm grating had a total area of $\sim 1.5 \times 10^5$ count-pixels. The relative efficiency of the two systems was thus $\sim 30\%$.

This can be understood as follows. The 3600 g/mm grating is reported by the manufacturer to be $\sim 30\%$ efficient in the region around 250 nm, while the 300 g/mm grating is reported to be $\sim 70\%$ efficient. Furthermore, the face normal of the 300 g/mm grating is at an angle of $\sim 2^\circ$ with respect to the long axis of the spectrometer, while the angle is 24° for the higher groove density grating. We thus expect the ratio of efficiencies to be

$$\text{Efficiency} \approx \frac{30 \cos(24)}{70 \cos(2)} = 39\%.$$

This accounts for most of the measured reduction in signal level with the high dispersion grating. The efficiency of the 3600 g/mm grating could be improved by a factor of ~ 2 if an ion-etched grating were used instead of the current grating.

A second dilemma with this system is related to the lack of an absolute wavelength calibration. The best solution to this problem is to have opposing views,¹ so that the line shift can be measured independent of the line center. HSX does not at present have any such views, although ideas have been suggested.⁵

A third difficulty associated with the system is related to the small flow velocities. The flow speeds of 10km/s noted above correspond to a line shift of only a single pixel. While the Gaussian fitting is certainly capable of localizing the line center to within a fraction of a pixel, the flows that might exist in the core of the standard discharges appear to be too small for easy measurement with this system. It is possible that higher ECH power operation will mitigate this problem to some extent, if the flow speeds and electric fields scale up with the input power.

In summary, Doppler flow measurements have been shown to work in principle in HSX. More effort is required to make the system a standard part of HSX operation.

¹ D.J. Den Hartog and R.J. Fonck, Rev. Sci. Instrum. **65**, 3238 (1994)

² Wavelength of 228.8022 nm taken from NIST database at http://physics.nist.gov/cgi-bin/AtData/main_asd.

³ BHK 89-9020-22 lamp, with BHK analamp power supply.

⁴ K.M. Likin, A. Abdou, A.F. Almagri, D.T. Anderson, F.S.B. Anderson, et al., Plasma Phys. Control. Fusion **45**, A133 (2003).

⁵ Private communication with A.F. Almagri.